# Hot Dust Close to the Young Massive Star Herschel 36

**B. Stecklum**[1], **T.L. Hayward**[2], **and P. Hofner**[3]

[1] Thüringer Landessternwarte, D-07778 Tautenburg
[2] Center for Radiophysics & Space Research, Cornell University, Ithaca
[3] University of Puerto Rico & Arecibo Observatory

**Abstract.** The O7 star Herschel 36 is responsible for the ionisation of the "hourglass" region in M 8. Adaptive optics near-infrared observations with ADONIS confirmed its association with compact diffuse emission. This feature is most likely due to scattered light and thermal radiation from dust grains which are situated very close to the massive star. Mid-infrared and radio continuum observations strongly support this view. These findings are discussed in the framework of possible explanations:
- Another proplyd-type object close to Herschel 36,
- A deeply embedded massive protostar close to the line of sight towards Herschel 36,
- Disk debris left from the formation of the high-mass star,
- An evaporating gaseous globule close to the O star.

## 1 Introduction

Herschel 36 (Her 36, HD 164740) is the most massive member of the young star cluster NGC 6523 situated in the western part of the H II region M 8, the Lagoon Nebula. It is of spectral type O7 V (Woolf 1961) and responsible for the ionisation of the "hourglass" nebula, the region of most conspicuous surface brightness in M8. The OB star cluster NGC 6530 is located at the centre of the giant H II region. The study of Van den Ancker *et al.* (1997) yielded its distance of 1.8 kpc and age of $\sim 10^7$yrs. From this region, sequential star formation spread towards the west leading to the formation of NGC 6523. Therefore, it seems reasonable that Her 36 is considerably younger than NGC 6530 while being at the same distance as this cluster.

Photometric and polarimetric investigations yielded clear evidence that this early-type star shows several peculiarities. It is considerably reddened ($(H-K) = 0.75, (K-L) = 1.41$, Whittet & van Breda 1980), a fact that raised the question whether its colour indices are due to an abnormal extinction law (R$= A_V/E_{B_V} = 5.0$, Clayton & Cardelli 1988) similar to that found in other regions of high-mass star formation, or due to an intrinsic infrared excess. Such an infrared excess could be caused by the thermal emission of hot dust grains close to the O star. A first sign for the presence of *circumstellar* dust was found by polarimetric investigations. The rotation of the orientation of the electric vector from $\Theta_{JHK} = 97°$ in the near-infrared to $\Theta_L = 28°$ at 3.6 $\mu$m can only be explained by a change of the scattering geometry with the varying optical depth (Wilking *et al.* 1988, Jones 1990).

First direct evidence for compact diffuse emission associated with Her 36 was gained by a lunar occultation observation in the $L'$ band (Stecklum *et al.* 1994). Subsequent speckle and adaptive-optics imaging as well as deconvolution of archival HST-WFPC images confirmed this finding (Stecklum *et al.* 1995). The discussion of these results emphasised a jet emerging from Her 36 as the possible cause, an explanation which has to be revised in the light of the new observations presented below.

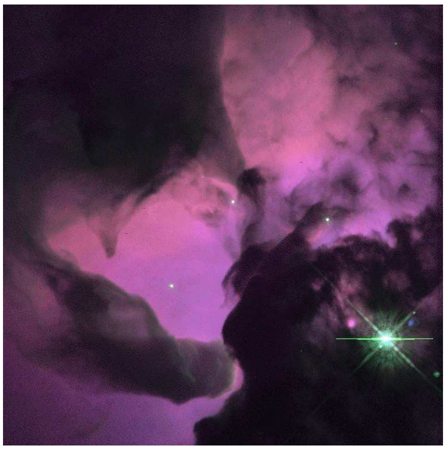

**Fig. 1.:** HST-PC2 true colour image of Her 36 and the hourglass.

The optical appearance of Her 36 and the hourglass region is illustrated in Fig.1 which shows a true-colour image composed of HST planetary camera frames. The field-of-view is 36$''$.8 by 36$''$.8 at the pixel scale of 0$''$.046. The image is rotated by -56° with respect to the equatorial coordinates. It clearly shows dense dust filaments even in the immediate neighbourhood of Her 36 which is the bright star to the lower-right. The purple spot next to Her 36 is the ultracompact HII region G5.97−1.17, the first proplyd-type object identified in a region of high-mass star formation other than the Orion Trapezium (Stecklum *et al.* 1998).

Her 36 is situated at the border of the distribution of the 2 cm radio continuum emission (Stecklum *et al.* 1998). Thus, its physical location is presumably very close to the boundary of the ionised bubble which expands into the dense molecular cloud core (Richter *et al.* 1998). This also suggests the occurrence of dust close to the O star.

## 2 Observations

This section summarises those observations from our extensive study of Her 36 and the Hourglass region which are of relevance to the topic of the present paper. Near-infrared (NIR) adaptive optics (AO) imaging of Her 36 in the wavelength range 1−2.3 $\mu$m ($JHK'$ bands) was carried out on August 7th 1995 using ESO's ADONIS system (Beuzit *et al.* 1994) equipped with the SHARP II camera (Hofmann *et al.* 1995)*. Her 36 ($V = 10.3$ mag, Johnson 1967) served as wavefront reference. Dithered frames at the pixel scale of 0$''$.05 were taken in order to mosaic the central region of M 8 at high spatial resolution. Aperture photometry was performed on these images (Richter 1996), and the results will be reported elsewhere (Richter *et al.* 1998). For their use in the present paper, the $JHK'$

* Based on observations collected at the European Southern Observatory, La Silla, Chile. Proposal-IDs 55.C-0674, 57.C-0515

AO images were deconvolved using the Richardson-Lucy algorithm (Richardson 1992; Lucy 1974).

Imaging in the $L$ band (3.5 $\mu$m) was obtained by AO observations using ADONIS in combination with the COMIC camera (Feautrier *et al.* 1995). The measurements were carried out on May 8th 1996 using a pixel scale of $0\farcs1$, and were part of a polarimetric investigation of Her 36 which aimed at the exploration of the scattering geometry. Although the spatial variation of the thermal background introduced by the ADONIS optics (see paper by H. Geoffray, this volume) prevented the derivation of a polarisation map, the integrated (*i.e.,* intensity) images are nevertheless useful.

The 11.7 $\mu$m image was obtained with SpectroCam-10, the Cornell-built 8-13 $\mu$m spectrograph/camera (Hayward *et al.* 1993) on the 5 m Hale telescope**. SpectroCam's detector is a Rockwell 128×128 Si:As BIB array. In camera mode, the pixel scale is $0\farcs25$ with a field of view of about $16'' \times 16''$.

The Hourglass region of M 8 was subject to imaging with the HST Planetary Camera. These observations were part of the WFPC2 IDT GTO program. The optical narrow- and broad-band images taken with WFPC2 (data sets U2O80xxxT) were retrieved from the ST-ECF archive after the one year proprietary period expired***.

Radio continuum measurements with the VLA† in A configuration were performed in 1996 December to map Her 36 at 2 cm wavelength at the highest angular resolution attainable with this interferometer.

## 3 Reduction of Adaptive Optics Imaging

Although a nearby star was imaged for point-spread-function (PSF) purposes during the adaptive optics observations of Her 36, the application of these reference images to remove the seeing halo by deconvolution did not yield the expected results. Thus, one can conclude that the intermittent imaging of the PSF reference star did not sample properly the variation of the seeing conditions.

Since Her 36 is surrounded by numerous stars of the young dense cluster, an iterative blind deconvolution scheme (e.g., IDAC, Jefferies & Christou 1993) seemed to be suited to circumvent the above problem. However, this attempt also failed because Her 36 is much brighter than any other star in the field. Thus, a two-step approach was chosen which finally yielded the intrinsic PSF

** Observations at the Palomar Observatory were made as part of a continuing collaborative agreement between the California Institute of Technology and Cornell University.

*** Based on observations made with the NASA/ESA Hubble Space Telescope, obtained from the data archive at the Space Telescope Science Institute. STScI is operated by the Association of Universities for Research in Astronomy, Inc. under the NASA contract NAS 5-26555.

† The National Radio Astronomy Observatory is a facility of the National Science Foundation operated under cooperative agreement by Associated Universities, Inc.

to a satisfying accuracy (better than that provided by the original PSF reference). For this purpose, the centroid position and peak intensity of each star was estimated using the appropriate DAOPHOT routines. Then, in an intermediate step, Her 36 was cut from the image and these pixels were set to the level of the background. This modified image served as input to a deconvolution process together with an artificial image build from $\delta$ functions at the locations of the cluster stars with peak heights corresponding to the previously derived intensities. This $\delta$-peak image served as PSF in this intermediate stage which, finally, yielded the "intrinsic" PSF of the original image. This intrinsic PSF was then applied in the deconvolution of the original image (including Her 36). For completeness, we add that these steps were performed on frames resampled to a finer grid (half the initial pixel size) to allow for more spatial frequencies which reduces the artifacts common to deconvolution algorithms.

## 4 Results

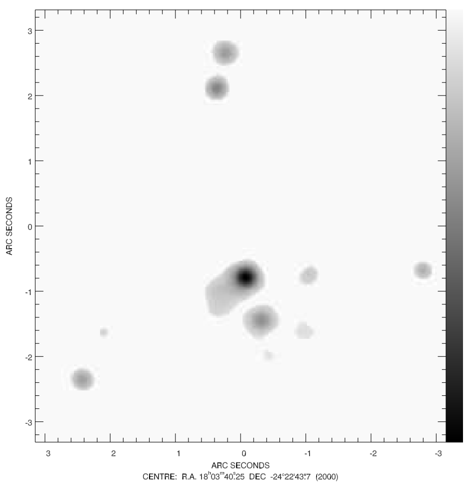


**Fig. 2.:** $K'$ image of Her 36 using a *fourth* root intensity scale.

The K' image resulting from 100 iterations of the Richardson-Lucy deconvolution is shown in Fig.2. It was re-convolved with a Gaussian to match the diffraction-limited angular resolution of 0.″15 which corresponds to a linear scale of 270 AU at the distance of 1.8 kpc. In order to display the the faint diffuse emission next to Her 36, a fourth root intensity scale was used. This feature has an angular extent of about ∼0.″8 or a projected linear size of ∼1500 AU. It was not detected in the J and H images.
The northern component of the binary star 3.″3 north of Her 36 was clearly detected in the $K'$, $L$, and 11.7 $\mu$m images and has a point-like appearance at these wavelengths. Therefore, is is very well suited as relative astrometric reference.

The $L$ image is displayed in Fig.3 using a linear intensity scale. It is the result of the superposition of the images taken at four orientations of the polariser using a shift-and-add routine. Contrary to $K'$, the image taken in the $L$ band was not subject to deconvolution. The high Strehl ratio of the $L$ image is obvious from the appearance of the first Airy ring. Note that the strength of the diffuse emission increased considerably compared to the brightness of Her 36. Also, contrary to the $K'$ image, the feature seems to be detached from Her 36 by about 0.″3 which corresponds to a projected linear separation of 500 AU. The bridging between Her 36 and the peak of the emission feature in the $K'$ band might be an artifact from the deconvolution process.

Fig.4 is a true-colour image constructed from the $K'$ (blue), $L$ (green), and 11.7 $\mu$m (red) frames. The binary component mentioned above was used for the proper registration of the images. The diffraction-limited angular resolution of each individual image was retained. Thus, stars appear bluish surrounded by a green halo (if bright enough in the $L$ band). The mid-infrared (MIR) emission is more wide-spread and peaks at the location of the maximum in the $L$ band. Obviously, in the MIR, the thermal emission from hot dust grains dominates over the photospheric flux from the O star.

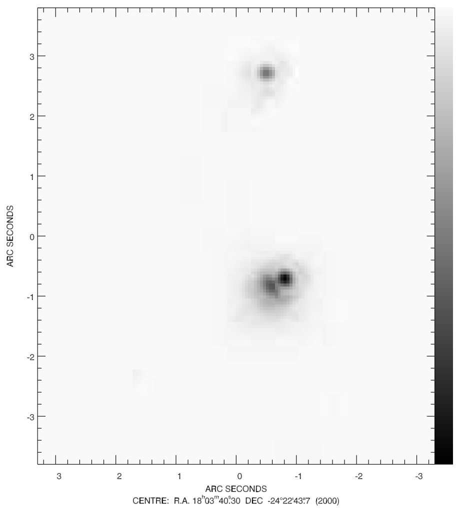


**Fig. 3.:** $L$ image of Her 36 using a *linear* intensity scale.

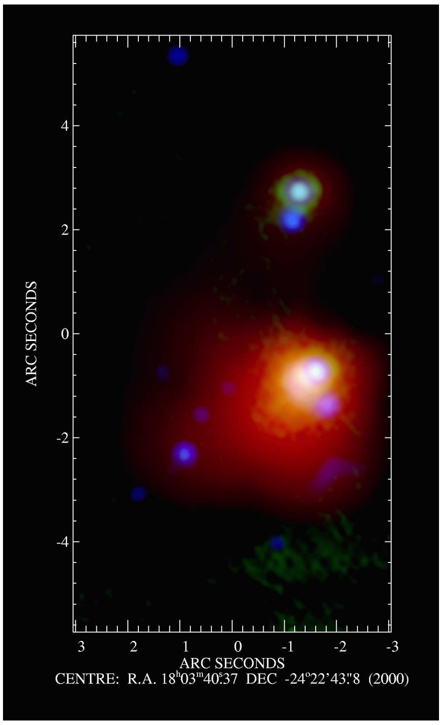


**Fig. 4.:** True colour image of Her 36 constructed from the $K'$ (blue), $L$ (green), and 11.7 $\mu$m (red) frames.

Finally, Fig.5 shows the WFPC2 H$\alpha$ image of Her 36 after subtraction of a point source modelled with TinyTim (Krist 1995). Although this subtraction was not perfect (some residuals remained at the position of the central peak), an emission feature $0\farcs3$ south-east of Her 36 became obvious which coincides with the peak of the thermal infrared radiation. The figure also shows the contour lines of the 2 cm radio continuum emission. In the radio continuum, a source was detected at the same location. The elliptical shape of the contours only reflects the VLA beam, the emission remained unresolved.

The main observational facts established from these measurements are as follows:

Close to the line of sight to Her 36, a source of intense infrared emission was found. It also emits optical emission lines and is a radio continuum source. The physical origin of this emission can be attributed to hot dust in an ionised gas in the immediate neighbourhood of Her 36. Although Her 36 seems to be responsible for the ionisation of the gas and the heating of the dust grains, the feature itself does not resemble a stellar jet emerging from the O star as it was claimed by Stecklum *et al.* (1995). The observations at high spatial resolution revealed that many if not all peculiarities attributed to Her 36 are in fact caused by the nearby infrared source.

## 5 Discussion

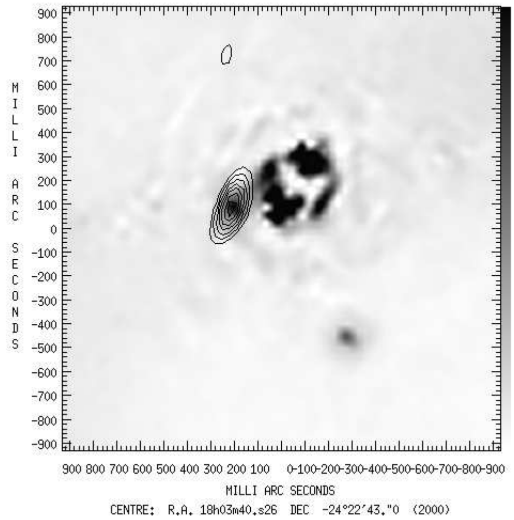


**Fig. 5.:** WFPC2 H$\alpha$ image of Her 36 after PSF subtraction with superimposed contour lines of the 2 cm radio continuum.

The spectral energy distribution of the infrared source close to Her 36 suggests the presence of dust grains at temperatures of $\sim 350\,K$. Assuming optically thin emission, the 11.7 $\mu$m flux can be caused by a total dust mass of about $4 \times -3$ Earth masses. The weak radio continuum flux indicates that a substantial fraction of the Lyman photons from Her 36 are being absorbed by dust rather than hydrogen.
Several possibilities exist to explain the observed properties of the infrared source. First of all, it seems unlikely that G5.97−1.17 is the only proplyd close to Her 36. Detailed inspection of the WFPC2 H$\alpha$ frames led to the detection of other proplyd candidates (Richter *et al.* 1998). However, since no central star at the peak position of the infrared source was found in the $JHK'$ images, we consider this explanation as unlikely.
The infrared source might represent a deeply embedded massive young stellar object which is, by chance, close to the line of sight to Her 36. This implies that both heating and ionisation are caused by the internal energy source rather than the external radiation field. However, such luminous objects are generally associated with masers ($H_2O$, OH, methanol; Hofner & Churchwell 1996, Caswell 1997). Since no masers are known close to the location of the infrared source, this hypothesis has to be questioned as well.
The youth of Her 36 suggests that the features discussed above might be caused by heated circumstellar matter, left from the formation of the massive star (disk debris). Although at this moment, this possibility cannot be strictly ruled out, the asymmetric distribution of the observed emission with respect to Her 36 renders it not very likely.
On the other hand, the photoevaporation of nearby dense molecular matter will lead to similar observational consequences known as partially ionised globule (PIG) or evaporating gaseous globule (EGG). Such a possibility is indicated by

the proximity of the ionisation front separating the plasma bubble ionised by Her 36 from the molecular cloud core. Furthermore, one might consider a relative motion of Her 36 with respect to the core. This, in turn, would imply that the observed feature is a transient phenomenon and might vary on rather short time scales.

The instrumentation becoming available at the ESO-VLT (especially CONICA) will allow the continuation of this study at much higher sensitivity and at least twice the angular resolution compared to that attainable with the 3.6-m telescope. These measurements will finally reveal which of the reasons sketched above actually leads to the observed phenomena. Our investigation showed that Her 36 is exceptionally well-suited to explore the influence of new-born high-mass stars on their natal environment.

## References


Caswell, J.L., 1997, MNRAS, 289, 203

Beuzit, J.L., Hubin, N., Gendron, E., Demailly, L., Gigan, P., Lacombe, F., Chazallet, F., Rabaud, D., & Rousset, G. 1994, in: *Adaptive Optics in Astronomy*, eds. M.A. Ealey & F. Merkle, Proc. SPIE, 2201 955

Clayton & Cardelli 1988, AJ, 96, 695

Feautrier, P., Beuzit, J.L., Lacombe, F., Petmezakis, P., Geoffray, H., Monin, J.L., Talureau, B., Gigan, P., Hubin, N., & Audaire, L. 1995, in: *Infrared Spaceborne Remote Sensing III*, eds. M.S. Scholl & B.F. Andresen, Proc. SPIE, 2553 208

Geoffray, H. 1998, in: *ESO/OSA Topical Meeting on Astronomy with Adaptive Optics*, this volume

Hayward, T.L., Miles, J.W., Houck, J.R., Gull, G.E., & Schoenwald, J. 1993, in: *Infrared Detectors and Instrumentation*, ed. A.W. Fowler, Proc. SPIE, 1946, 334

Hofner, P. & Churchwell, E. 1996, A&AS, 120, 283

Jefferies, S.M. & Christou, J. 1993, ApJ, 415, 862

Johnson, H.L. 1967, ApJ, 147, 912

Jones, T.J. 1990, AJ, 99, 1894

Krist, J. 1995, in: *Astronomical Data Analysis Software and Systems*, eds. R.A: Shaw, H.E. Payne & J.J.E. Hayes, ASP Conf. Ser. 77, 349

Lucy, L.B. 1974, AJ, 79, 745

Richardson, W.H. 1972, JOSA, 62, 55

Richter, S., Stecklum, B., Henning, Th., & Launhardt, R. 1998, in preparation

Richter, S. 1996, M.A. Thesis, University Jena

Stecklum, B., Henning, T., Feldt, M., Hayward, T.L., Hoare, M.G., Hofner, P., & Richter, S. 1998, AJ, 115, 767

Stecklum, B., Henning, T., Eckart, A., Howell, R.R., & Hoare, M. 1995, ApJ, 445, L153

Stecklum, B., Howell, R.R., T., Eckart, A., & Richichi, A. 1994, in: *IAU Symp. 158, Very High Angular Resolution Imaging*, ed. J.G. Robertson & W.J. Tango (Dordrecht: Kluwer), 364

Van den Ancker, M.E., Thé, P.S., Feinstein, A., Vázquez, R.A., Winter, D. de, & Pérez, M.R. 1997, A&AS, 123, 63

Wilking, B.A., Lebofsky, & P.G., Rieke 1982, AJ, 87, 695

Whittet & van Breda 1980, MNRAS, 192, 467

Woolf, N.J. 1961, PASP, 73, 206